Facilitating pyramid to horizontal oriens–alveus interneurone inputs: dual intracellular recordings in slices of rat hippocampus

Afia B. Ali and Alex M. Thomson

Department of Physiology, Royal Free Hospital School of Medicine, Rowland Hill Street, London NW3 2PF, UK

(Received 26 September 1997; accepted after revision 18 November 1997)

1. In adult rat hippocampal slices, simultaneous intracellular recordings from pyramidal cells in CA1 and interneurones near the stratum oriens–alveus border revealed excitatory connections that displayed facilitation on repetitive activation in twelve of thirty-six pairs tested.

2. Postsynaptic interneurones were classified as horizontal oriens–alveus interneurones by the pronounced 'sag' in response to hyperpolarizing current injection, high levels of spontaneous synaptic activity and by the morphology of their somata and dendrites, which were confined to stratum oriens–alveus and their axons which projected to stratum lacunosum-moleculare where they ramified extensively, in the region of entorhinal cortex input to CA1.

3. Excitatory postsynaptic potentials (EPSPs) elicited by single pyramidal cells were 0 to 12 mV in amplitude. Mean EPSP amplitude (single spikes) was $0{\cdot}93 \pm 1{\cdot}06$ mV at $-70 \pm 2{\cdot}3$ mV ($n = 10$). The rise time was $1{\cdot}2 \pm 0{\cdot}5$ ms and the width at half-amplitude was $7{\cdot}5 \pm 4{\cdot}7$ ms.

4. EPSPs fluctuated greatly in amplitude; the mean coefficient of variation was $0{\cdot}84 \pm 0{\cdot}37$ for the first EPSP and $0{\cdot}47 \pm 0{\cdot}24$ for the second. Apparent failures of transmission frequently occurred after first presynaptic spikes but less frequently after the second or subsequent spikes in brief trains.

5. EPSPs displayed facilitation at membrane potentials between −80 mV and spike threshold. Second EPSPs within 20 ms of the first were 253 ± 48% (range, 152–324%) of the mean first EPSP amplitude. Third EPSPs within 60 ms were 266 ± 70% (range, 169–389%) and fourth EPSPs within 60–120 ms were 288 ± 71% (range, 188–393%). Both proportions of apparent failures of transmission and coefficient of variation analysis indicated a presynaptic locus for this facilitation.

Previous anatomical studies (e.g. Ramón y Cajal, 1911) describe several classes of interneurones in the hippocampus which may be segregated into categories according to their immunoreactivity for calcium binding proteins and peptide neurotransmitters and their axonal and dendritic arborization (Freund & Buzsáki, 1996). Axons of interneurones often target specific domains of pyramidal cells; some contact pyramidal cells perisomatically, others terminate on their dendrites (e.g. Gulyás, Miles, Hájos & Freund, 1993; Buhl, Halasy & Somogyi, 1994; Sík, Penttonen, Ylinen & Buzsáki, 1995; Freund & Buzsáki, 1996; Halasy, Buhl, Lorinczi, Tamas & Somogyi, 1996). This anatomical diversity is thought to result in functional diversity (Li, Somogyi, Tepper & Buzsáki, 1992; Buhl, Han, Lorinczi, Stezhka, Karnup & Somogyi, 1994; Miles, Tóth, Gulyás, Hájos & Freund, 1996; Buhl, Szilágyi, Halasy & Somogyi, 1996). In addition to the more widely studied interneurones with their somata in the cell body layer and those whose somata are in stratum (s.) radiatum and s. lacunosum-moleculare, there are at least two broad classes of oriens–alveus (O–A) interneurones, the vertically and horizontally oriented cells. The vertically oriented O–A interneurones have dendrites that extend vertically and horizontally in the oriens and into s. radiatum and s. lacunosum-moleculare and axons that innervate s. pyramidale (McBain, Dichiara & Kauer, 1994). Horizontal O–A interneurones in CA1 with somata located at the O–A border are an anatomically distinct class of interneurones with horizontally oriented sparsely spiny dendrites confined to s. oriens and alveus. Where reconstruction has been possible the axons of these cells were shown to project to s. lacunosum-moleculare, the region of entorhinal cortex input to CA1, and to ramify there extensively (Ramón y Cajal, 1911; Lacaille, Mueller, Kunkel, Schwartzkroin, 1987; Lacaille & Williams, 1990; Buckmaster, Kunkel, Robbins &

Schwartzkroin, 1994; Blasco-Ibanez & Freund, 1995). Preliminary evidence suggests that these cells have little direct effect upon the somatic excitability of pyramidal cells, but may inhibit distal dendritic inputs (Yanovsky, Sergeeva, Freund & Haas, 1997). So far two subclasses of horizontally oriented O–A interneurones have been identified immunocytochemically. Most of these interneurones contain somatostatin (Morrison, Benoit, Magistretti, Ling & Bloom, 1982; Kosaka, Wu & Benoit, 1988; Kunkel & Scwartzkroin, 1988), but a smaller number are immunoreactive for calbindin (Toth & Freund, 1992). The calbindin-immunoreactive cells are thought to project to the medial septum (Toth, Borhegyi & Freund, 1993). The somatostatin-containing horizontal O–A interneurones which innervate s. lacunosum-moleculare, also express a high level of metabotropic glutamate receptor 1α (mGluR1α) in soma and dendrites. A high level of metabotropic glutamate receptor 7 (mGluR7) is seen in the presynaptic axon terminals contacting these cells, i.e. probable presynaptic autoreceptors (Shigemoto *et al.* 1996). Anatomical studies show that these cells are densely innervated by CA1 pyramidal cells (Blasko-Ibanez & Freund, 1995) and Lacaille *et al.* (1987) reported paired recordings in which pyramidal cells elicited EPSPs in O–A interneurones. However, these O–A interneurones typically innervated s. pyramidale, could elicit IPSPs that were recordable in pyramidal somata and had some dendrites that extended into s. radiatum. The functional properties of the dense connections from pyramidal cells to horizontal O–A interneurones have not been studied in any detail.

Postsynaptic responses to brief trains of presynaptic spikes have been shown to display frequency-dependent facilitation or frequency-dependent depression, depending, apparently, on the postsynaptic target neurone. Invertebrate studies show that different axon terminals of the same motoneurone exhibit different activity-dependent release properties, i.e. depression occurs at one synapse on one target and facilitation at another (e.g. Katz, Kirk & Govind, 1993). Paired intracellular recordings in neocortex have demonstrated that excitatory connections from pyramidal cells to certain classes of neocortical interneurones display pronounced frequency-dependent facilitation (Thomson, Deuchars & West, 1993*a*, 1995). In contrast, pyramidal inputs to other classes of interneurones and to other pyramidal cells typically display depression, both in neocortex (Thomson, Deuchars & West, 1993*b*; Markram & Tsodyks, 1996) and in the CA1 region of the hippocampus (Deuchars & Thomson 1996). However, in neocortex it is difficult to classify interneurones precisely on the basis of their gross morphology. No equivalent comparison of the frequency-dependent properties of synapses made by pyramidal axons with the more readily identified interneurones in CA1 has yet been performed. In this study therefore paired intracellular recording and biocytin filling were used to determine the frequency dependence of transmitter release at excitatory connections made by pyramidal axons with horizontally oriented O–A interneurones of the CA1 region of the adult rat hippocampus. Preliminary reports of these data have appeared (Ali & Thomson, 1996, 1997).

METHODS

Male Sprague–Dawley rats, 90–150 g in weight, were anaesthetized with Fluothane followed by an intraperitoneal injection of sodium pentobarbitone (60 mg kg^{-1} Sagatal; Rhone Merieux, France). The rats were then perfused transcardially with 50–100 ml ice-cold artificial cerebrospinal fluid (ACSF) with added sodium pentobarbitone (60 mg l^{-1}). Perfusion ACSF contained (mM): 248 sucrose, 25·5 $NaHCO_3$, 3·3 KCl, 1·2 KH_2PO_4, 1·0 $MgSO_4$, 2·5 $CaCl_2$ and 15 D-glucose at 34–35 °C and was equilibrated with 95% O_2–5% CO_2. The animals were decapitated and 450–500 μm coronal sections of the brain including the hippocampus were cut using a Vibroslice (Camden Instruments, UK). The slices were maintained at the interface between ACSF and warm, humidified 95% O_2–5% CO_2 at 34–35 °C. The slices were incubated in the sucrose-containing ACSF for the first hour. This was then replaced with ACSF containing (mM): 124 NaCl, 25·5 $NaHCO_3$, 3·3 KCl, 1·2 KH_2PO_4, 1·0 $MgSO_4$, 2·5 $CaCl_2$ and 15 D-glucose at 34–35 °C, in which all recordings were performed.

Electrophysiological recordings

Paired recordings were performed using conventional sharp electrodes (resistance, 80–160 MΩ) containing 2 M potassium methylsulphate and 2% biocytin (w/v) under current clamp conditions, using an Axoprobe amplifier (Axon Instruments). The search strategy for connected pairs involved first obtaining a stable intracellular recording from one pyramidal neurone located in the cell body layer. A search was then made for an interneurone located at the oriens–alveus border. Trains of action potentials were elicited in the pyramidal cell by injection of square-wave current pulses delivered once every 3 s, and any voltage change in the interneurone was recorded. Any possible connection from the interneurone to the pyramid was also tested. If both tests were negative, a second pyramidal cell was penetrated and tested and so on. With connected pairs, continuous analog recordings from both neurones were made on magnetic tape (Racal, Store 4). Since spontaneous changes in membrane potential can affect postsynaptic responses, the postsynaptic membrane potential was held within a pre-set range ($\pm$1 mV) by continuous manual current clamp (injection of current to maintain a stable membrane potential) and then changed to another potential after sufficient data had been collected. Continuous monitoring/control of electrode balance was achieved by observing voltage responses to small brief current pulses injected into the postsynaptic cell before the response to presynaptic spikes. The electrophysiological characteristics of recorded cells were obtained from their voltage responses to 500 ms current pulses between −2 and +1 nA in amplitude (delivered from membrane potentials in the range −65 to −85 mV) using pCLAMP software (Axon Instruments).

Data analysis

Data that had been collected on analog tape were digitized (5–10 kHz; voltage resolution, 0·005–0·01 mV), stored on optical disc and analysed off-line (using in-house software). Individual sweeps were observed and either accepted, edited, or rejected according to the trigger points that would trigger measurements and averaging of the EPSPs during subsequent data analysis. Averaging of EPSPs was triggered by the rising phase of the first presynaptic spike for the first EPSP, the rising phase of the second presynaptic spike, for the second EPSP and so on (illustrated in Fig. 1). For the averages illustrated and measurements given,

individual records in which second, third, fourth and fifth spikes fell within a narrow time window (e.g. 14–20 or 35–40 ms) following the first spike were selected into data subsets and averaged. Standard deviation time course (SDTC) plots the standard deviation about the mean and indicates whether the time course of the EPSP fluctuates significantly from event to event.

Single spike or first spike EPSP amplitude was measured as the difference between the baseline and the peak of the EPSP. Where subsequent EPSPs were well separated in time, the same procedure was used. The amplitudes of second, third, fourth or fifth EPSPs that summed with preceding EPSPs were measured as the difference between the peak of that EPSP and the falling phase of the averaged preceding EPSP. An averaged first, second or third EPSP trace was scaled to match the amplitude of the equivalent single sweep event, superimposed on that event and the amplitude of the following EPSP was measured as the difference between its peak and the equivalent point on the falling phase of the scaled average. All these single sweep measurements were controlled by hand and sweeps containing large spontaneous postsynaptic events were excluded. Where no postsynaptic response was discernible, a measure of 0 mV was entered. The 'zero' bins in the histograms therefore indicate total apparent failures of transmission. Averaging of these sweeps produced no apparent EPSP. For c.v. (coefficient of variation) analysis, mean EPSP amplitudes and c.v.s were calculated from these measurements without corrections for noise distributions. The 10–90% rise time was measured as the time taken for the EPSP to rise from 10 to 90% of its peak amplitude. No correction was made for the possibility that presynaptic spike artifacts obscured the earliest part of the rising phase, so these measurements of rise time may be a slight underestimate. The width at half-amplitude was measured as the time interval between the EPSP to rising to 50% and falling to 50% of its peak amplitude. Numbers given in the text are means ± S.D.

Histological processing

Following the paired recording, cell pairs were filled with biocytin by passing 0·5 nA depolarizing current pulses in a 50% duty cycle at 1 Hz for 5–15 min. The slices were incubated for a further 5–15 min in the recording chamber after filling with biocytin, and were then fixed for 1 h in a solution of 0·1 M phosphate buffer containing 1·25% glutaraldehyde and 2·5% paraformaldehyde. Slices were then incubated in 20% sucrose in 0·1 phosphate buffer overnight. After embedding the sections in gelatin, they were sectioned at 60 μm on a Vibratome. Injected biocytin was localized using the Vector stain ABC Elite kit (Vector Laboratories, Peterborough, UK), incubated with 0·1% Triton overnight. The injected biocytin was then visualized using 3′,3′-diaminobenzidine

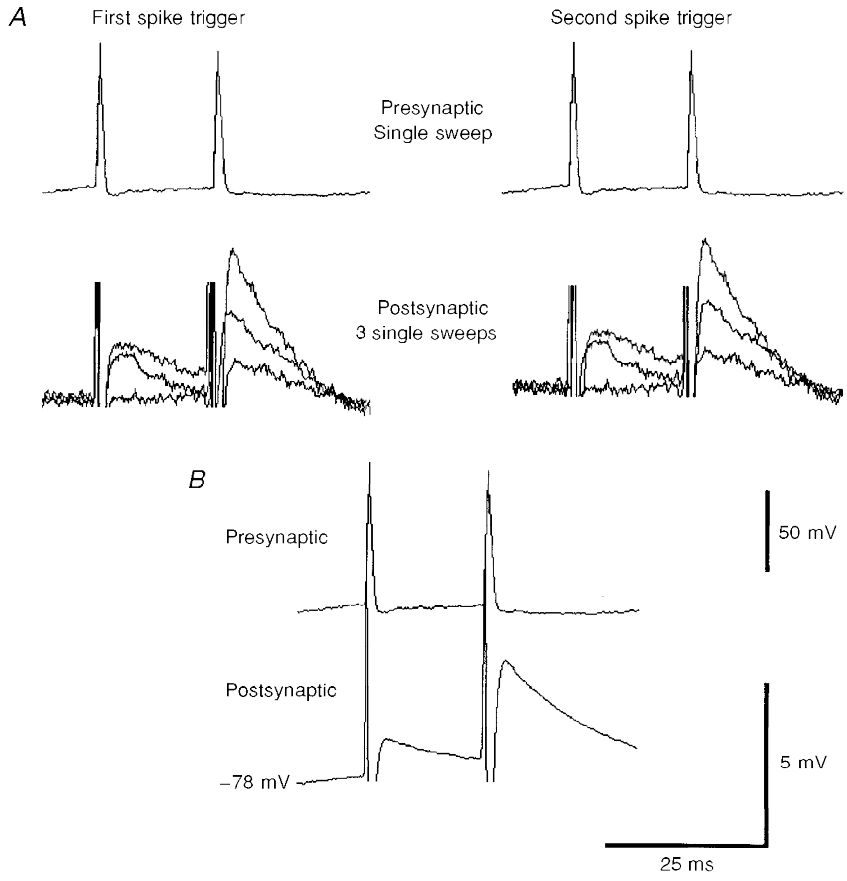

Figure 1. Raw data from a pyramid to horizontal O–A interneurone connection

A, single sweep EPSPs at −72 mV. Presynaptic action potentials (one sweep) are shown above. Due to the variation in the size of the EPSPs from sweep to sweep (lower records in *A*), an average was computed. Most of the EPSPs illustrated in subsequent figures are composite averages triggered from the rising phase of the first presynaptic spike for the first EPSP and the rising phase of the second spike for the second EPSP and so on. *B* shows the computed average. The spike artifacts visible here are removed graphically from other figures.

(DAB, Sigma) and the sections dehydrated and embedded in Durcupan resin (Fluka) on slides. Filled and recorded interneurones were fully reconstructed using a drawing tube under a ×100 objective lens.

RESULTS

Horizontal O–A interneurones were extremely difficult to find, impale and stabilize, probably due to their low packing density. However, during these experiments, thirty-six dual recordings in which a horizontal O–A interneurone was recorded simultaneously with a pyramidal cell were obtained and an EPSP was elicited in the interneurone by action potentials in the pyramidal cell in twelve of these pairs. This gave an average probability of finding a connection of 1:3, i.e. on average, each interneurone was tested with three pyramidal cells before a connection was found. Four of these pairs involved two postsynaptic interneurones that were each excited by two consecutively recorded pyramids. In none of these paired recordings was an inhibitory postsynaptic potential apparent in the pyramidal cell when the interneurone fired, even with bursts of five to eight interneurone spikes. Eight interneurones (postsynaptic cells in 10 pairs) were successfully filled with biocytin and fully reconstructed at the light microscopic level (×100 magnification). The other two interneurones included here displayed electrophysiological characteristics similar to those of identified horizontal O–A interneurones and quite distinct from those of vertically oriented O–A interneurones and of cell body layer interneurones (Ali, Deuchars, Pawelzik & Thomson, 1998).

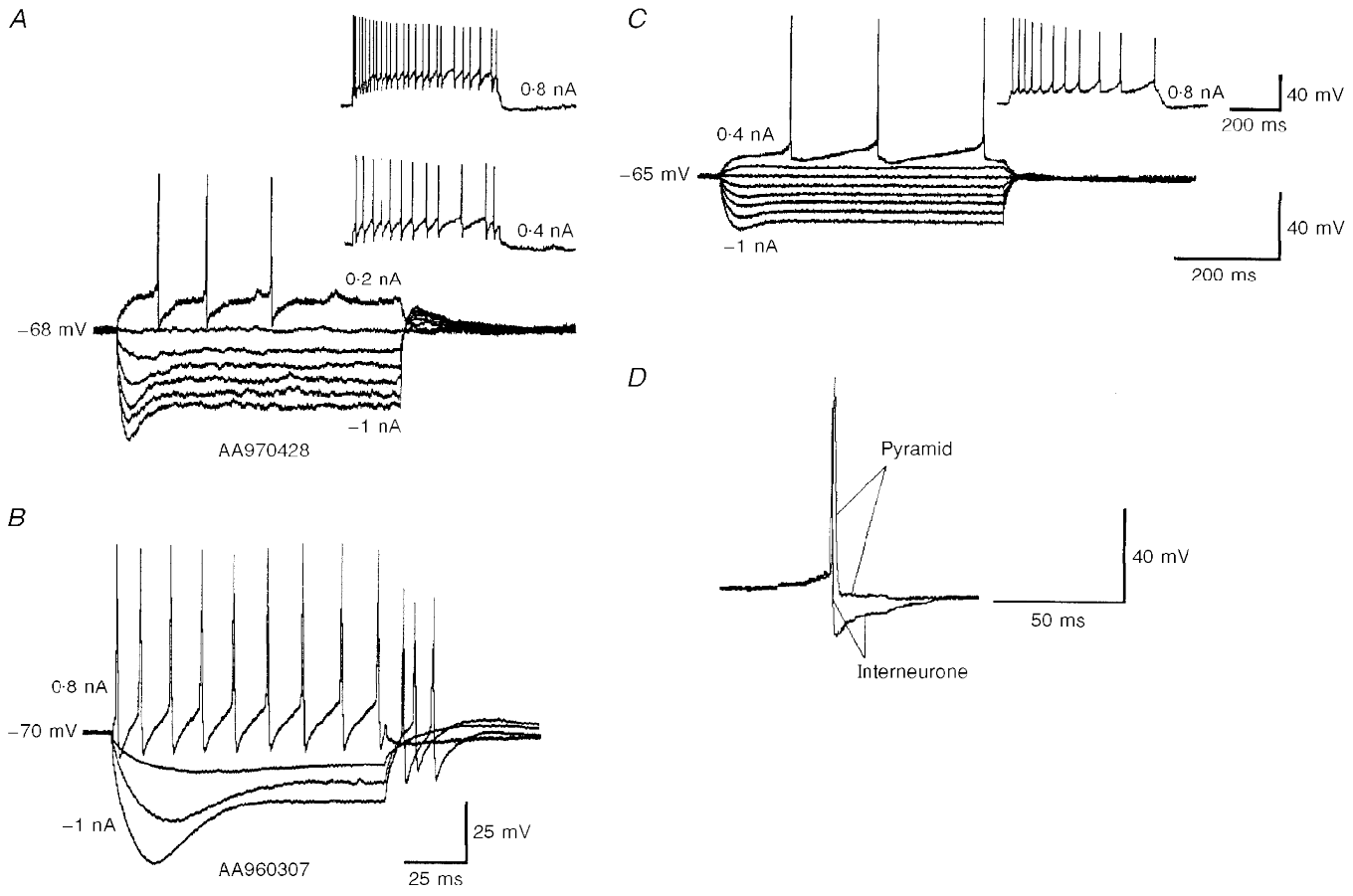

Figure 2. Electrophysiological characteristics of two horizontal O–A interneurones (*A* and *B*) and a pyramidal cell (*C*)

Voltage responses to depolarizing and hyperpolarizing current pulses are shown. The amplitude of the largest negative pulse and the largest positive pulse are given on each trace. Intervening current pulses are −0·8, −0·6, −0·4 and −0·2 nA, respectively (ascending order in *A* and *C*). For the cell in *B* the intervening pulses are −0·6 and −0·2 nA. Horizontal O–A interneurones displayed a pronounced 'sag' in the response to hyperpolarizing current injection, rebound depolarization after the pulse and little spike accommodation or frequency adaptation. A single pyramidal cell spike superimposed on a single horizontal O–A interneurone spike is shown in *D*. The interneurone spikes were faster than pyramidal spikes and were terminated by a larger after-hyperpolariztion (AHP). The scale bar for the superimposed spikes is shown on the right-hand side. The scale bars for *C* apply to *A*.

Electrophysiological characteristics of horizontal O–A interneurones

Figure 2 illustrates the response of a pyramidal cell and of two horizontal O–A interneurones to injected current pulses. The horizontal O–A interneurones were electrophysiologically distinct from the pyramidal cells in the briefer time course of their action potentials (width at half-amplitude, 0·6 ± 0·3 ms) and their large, fast spike after-hyperpolarizations (AHPs), which were 16·1 ± 10·7 mV in amplitude (spike threshold to AHP peak) with a width at half-amplitude of 6·58 ± 2·7 ms (shown in detail in Fig. 2*D*). The spike amplitudes were 58·75 ± 7·2 mV (overshoot, 8 ± 4·5 mV) and firing showed less spike frequency adaptation or accommodation than in pyramidal cells (Maccaferri & McBain, 1995; see Zhang & McBain, 1995*a,b* for complete description of K^+ currents associated with the spike AHP). The resting membrane potentials of the interneurones were between −65 and −85 mV. The input resistances measured from voltage responses to −0·2 nA current pulses were 70 ± 13·72 MΩ with a time constant of 12·8 ± 1·5 ms. The input resistance measured at the peak of the voltage response to a −1·0 nA hyperpolarizing current pulse delivered at −71·12 ± 10·4 mV was 47·2 ± 15·1 MΩ and at the end of the 500 ms current pulse the input resistance was 29 ± 11·34 MΩ. This pronounced 'sag' in the response to negative current injection and the subsequent rebound depolarization was a consistent electrophysiological characteristic of the horizontal O–A interneurones (as described previously, Lacaille & Williams, 1990; McBain, 1994; Sík *et al.* 1995; Maccaferri & McBain, 1996). Another consistent characteristic was the high frequency of spontaneous synaptic activity, 20·75 ± 8·0 Hz at rest

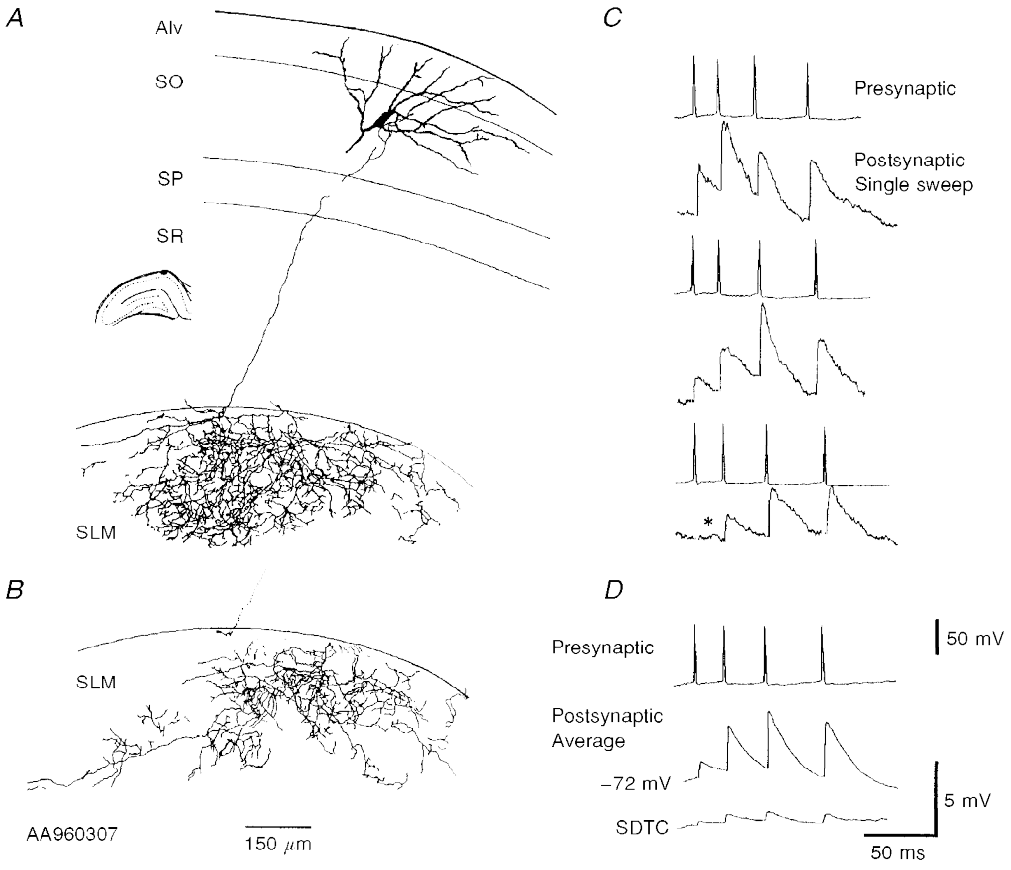

Figure 3. Morphology and single sweep EPSPs of a horizontal O–A interneurone

A and *B*, full reconstruction of a horizontal O–A interneurone drawn from three 60 μm transverse sections. The cell body was located in the O–A border, with horizontally oriented sparsely spiny dendrites confined to the oriens and the alveus (Alv). The axon projected from the cell body to s. lacunosum-moleculare, where it ramified extensively. SO, s. oriens; SP, s. pyramidale; SR, s. radiatum; SLM, s. lacunosum-moleculare. For simplicity the interneurone axon from only one of three 60 μm sections containing the axon is drawn in *A*, the remaining axon is drawn in *B* where the dotted line illustrates the relative position of the main axon. The current–voltage relation for this cell is shown in Fig. 2*A*. Three single sweeps (raw data) of the EPSPs elicited in this cell by a simultaneously recorded pyramid are shown in *C*. The single sweeps illustrate the variation in the size of the EPSPs from sweep to sweep and an apparent failure of transmission after the first presynaptic spike (third trace, *). The composite averaged EPSP (60–120 sweeps) and the SDTC (standard deviation time course) are shown in *D*.

(average peak amplitude of spontaneous EPSPs, 1·6 ± 0·8 mV; previously described by Lacaille *et al.* 1987; Lacaille & Williams, 1990). Pyramidal cell properties were similar to those reported previously (e.g. Deuchars & Thomson, 1996).

Morphology of horizontal O–A interneurones

The somata of the eight postsynaptic interneurones reported here were located in the superior zone of s. oriens close to the O–A border. Their sparsely spiny dendrites branched horizontally along s. oriens and the alveus, but did not extend as far as s. pyramidale. A single axon originated from the cell body, crossed s. pyramidale and ran through s. radiatum to s. lacunosum-moleculare, where it ramified extensively. No collaterals were observed outside s. lacunosum-moleculare, and the axon arborization and apparent boutons were confined to s. lacunosum-moleculare in seven of these interneurones. Figures 3, 4 and 5 illustrate examples of the morphology of horizontal O–A interneurones. In Fig. 3, for simplicity the axon shown in register with the soma and dendrites was reconstructed from only one of three 60 μm serial sections containing the axon. The axon illustrated in the adjacent drawing was reconstructed from the two neighbouring sections. The axon of the remaining postsynaptic interneurone (Fig. 5) densely innervated s. lacunosum-moleculare but one collateral also branched in s. oriens. These arbors are similar to those reconstructed from neurones filled *in vivo* (Sík *et al.* 1995).

Figure 4*A* illustrates the reconstruction of a horizontal O–A interneurone from a more longitudinal plane of section. The axonal arborization in s. lacunosum-moleculare in this plane of section was limited in comparison with the interneurones reconstructed from transverse sections. However, the dendrites extended further and ramified more extensively than those of other horizontal O–A interneurones. Whether this represents a subclass of horizontal O–A interneurones or whether the dendritic tree is generally more intact in this plane remains to be determined. It may, however, be interesting to note that this cell received the largest EPSP recorded in this study. A similarly large dendritic arbor and

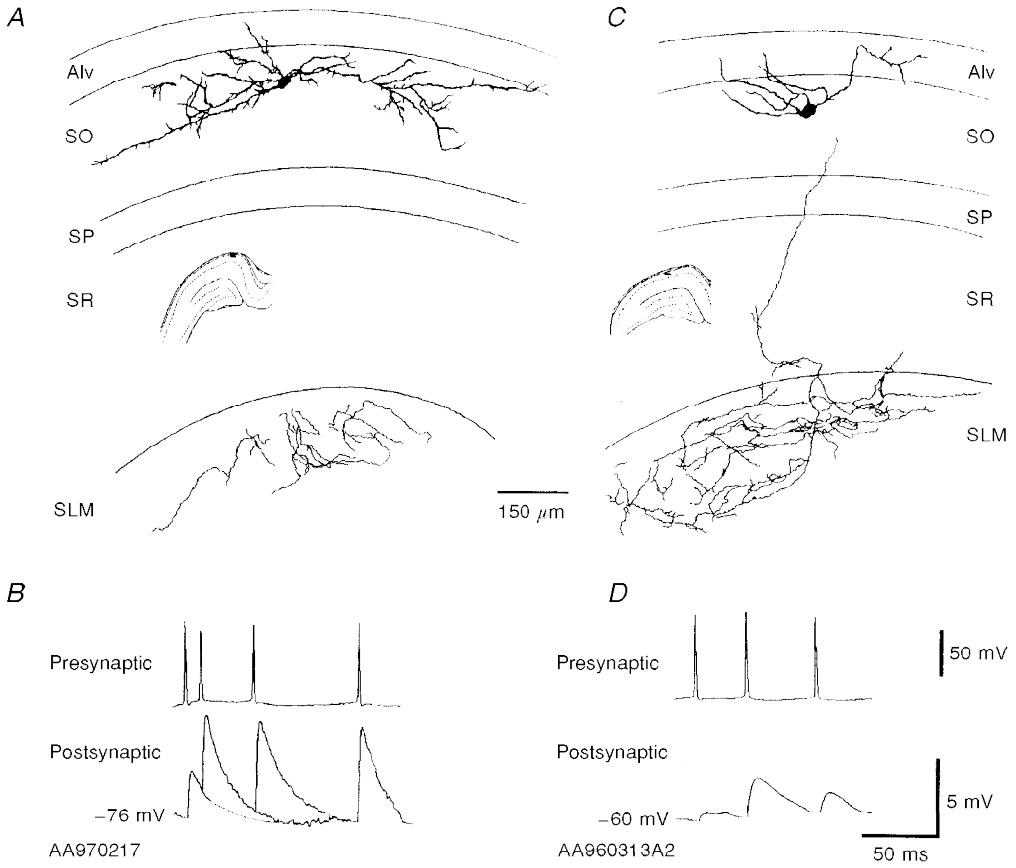

Figure 4. Morphology and synaptic responses of two horizontal O–A interneurones in different planes of section

A and *B*, two horizontal O–A interneurones are shown reconstructed from 2 different planes of section. These were the largest (*B*) and the smallest (*D*) first spike EPSPs recorded to date. The interneurone in *A* was reconstructed from a more longitudinally oriented section of hippocampus and the interneurone in *C* from a traditional transverse section. There was a difference in extent of the axonal and dendritic arborization in the two cells. Dendritic arborization is greater in the cell recorded in a more longitudinally oriented slice and axonal arborization greater in a transverse slice. The EPSPs elicited in both of these interneurones are shown below. The scale bar applies to both *B* and *D*.

limited axonal arbor were observed in the only other horizontal O–A interneurone histologically recovered from a more longitudinally oriented slice. However, no connections were recorded associated with this interneurone and it is therefore not included in the present study.

Amplitude and time course of pyramid to horizontal O–A interneurone EPSPs

From the twelve pairs studied, EPSPs generated by ten connections were analysed in detail. For these, in 2·5 mM Ca^{2+}, at a postsynaptic membrane potential of $-70 \pm 2{\cdot}30$ mV and with a presynaptic firing rate of 0·33 Hz, the mean amplitude of the EPSP elicited by the first presynaptic action potential was $0{\cdot}93 \pm 1{\cdot}06$ mV (range, 0·1–3·71 mV). The average first EPSP 10–90% rise time was $1{\cdot}2 \pm 0{\cdot}5$ ms (range, 0·6–1·8 ms), with a mean width at half-amplitude of $7{\cdot}5 \pm 4{\cdot}7$ ms (range, 2·6–12 ms). The standard deviation time course typically paralleled the shape of the averaged EPSP, indicating that the EPSPs did not fluctuate significantly in shape despite large fluctuations in amplitude. Figure 4 illustrates the largest and the smallest average first EPSPs recorded to date and Fig. 5, illustrates the variation in the time course and size of the EPSPs elicited in a single interneurone by two consecutively recorded pyramid cells.

Apparent failures of transmission

These EPSPs exhibited large sweep-to-sweep fluctuations in amplitude. In Figs 1, 3 and 12, examples can be seen of single sweep EPSPs obtained from pyramid to horizontal O–A interneurone connections. Apparent failures of transmission were commonly observed in these connections alternating with large EPSPs. They most frequently occurred following the first presynaptic spike, where an average apparent failure rate of $25{\cdot}8 \pm 15{\cdot}5$% (range, 11–49%, 5 connections, 10 data sets included) was observed. Second and third presynaptic action potentials gave rise only to $6{\cdot}1 \pm 9{\cdot}1$% and $5{\cdot}5 \pm 9{\cdot}3$% apparent failures, respectively (ranges, 0–22 and 0–25%, respectively). Apparent failures of transmission were observed following only $1{\cdot}5 \pm 3{\cdot}3$% of fourth presynaptic action potentials (10 data subsets) (see Fig. 6 for EPSP amplitude distributions).

Paired pulse and brief train facilitation

All twelve pyramid to horizontal O–A interneurone connections displayed paired pulse and brief train facilitation at 0·33 Hz (see Figs 1, 3–5 and 9–11). Averaged second EPSPs were between 2 and 5 times the amplitude of first EPSPs at interspike intervals < 20 ms. For five pairs it was possible to measure the amplitudes of sufficient single

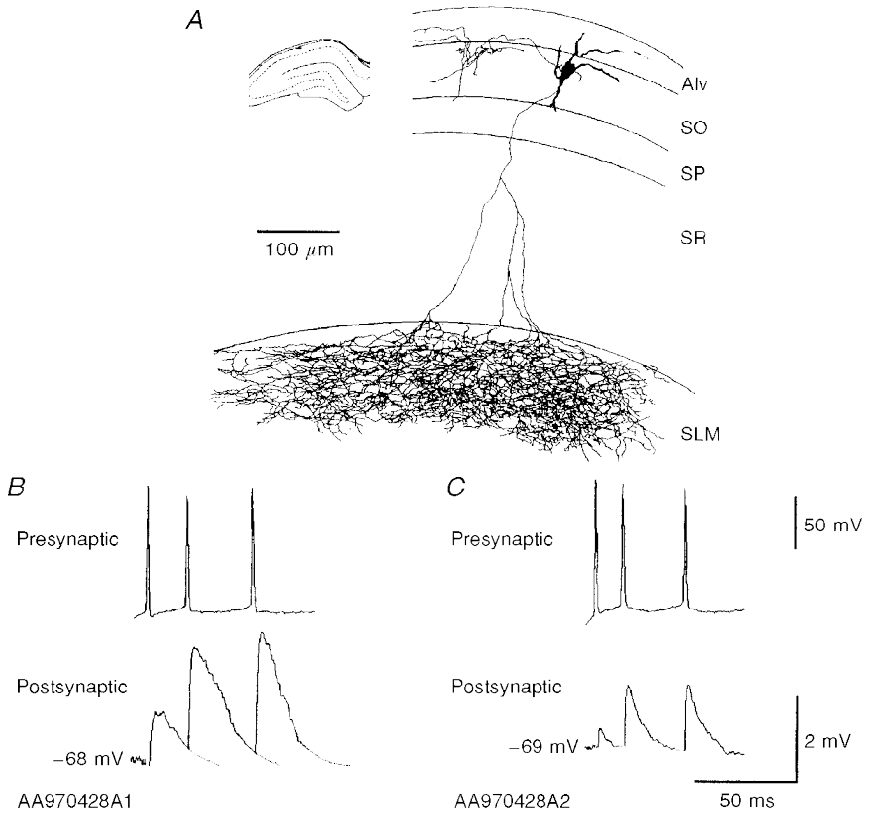

Figure 5. An interneurone that was postsynaptic to two consecutively recorded pyramidal cells

A, the axonal arborization was slightly different from the other 7 reconstructed interneurones in that it innervated s. oriens, albeit sparsely, as well as projecting to s. lacunosum-moleculare where it ramified extensively. The axon was reconstructed from four 60 μm thick sections. *B* and *C*, the amplitude and duration of the EPSPs differed between the two connections.

sweep events to obtain mean amplitudes and coefficients of variation (c.v.) for second, third and in some cases, fourth and fifth EPSPs occurring within narrow interspike interval ranges and at a constant membrane potential. These data subsets included > sixty events for first EPSPs, twenty to sixty single sweep events for second EPSPs, between fifteen and fifty for third EPSPs and between ten and forty for fourth EPSPs. For these data subsets, the mean amplitudes of second EPSPs occurring within 20 ms of the first were 253 ± 48 % (range, 152–324 %) of the mean first EPSP amplitude. Between 20 and 40 ms, second EPSPs were a little smaller, 214 ± 46 % of the first EPSP amplitude (127–264 %). Third EPSPs occurring within 60 ms of the first were 266 ± 70 % (range, 169–389 %) and fourth EPSPs occurring between 60 and 120 ms of the first were 288 ± 71 % (range, 188–393 %) of the mean first EPSP amplitude. Figure 7 plots these mean EPSP amplitudes against time interval and indicates the time course of facilitation.

The c.v.s for these EPSP amplitudes were typically large, 0·84 ± 0·37 (range, 0·14–1·58) for the first and 0·47 ± 0·24 (range, 0·19–0·92) for the second EPSP (26 data subsets), the largest c.v.s corresponding to the smallest average EPSPs, which included large proportions of apparent failures. Small differences in mean EPSP amplitude therefore do not reach significance with the numbers of sweeps included in many of these data sets and differences of <50 % may indicate a trend, but do not reach significance. The plot and regression lines illustrating the time course of facilitation (Fig. 7, 26 data subsets for second, 24 for third and 9 for fourth EPSPs) indicate a trend (see also averaged EPSPs in Figs 10 and 11), i.e. that, as previously described (Thomson, 1997), the facilitation (of second EPSPs) generated by a single preceding action potential is of briefer duration than the facilitation (of third and fourth EPSPs) which results from two or three preceding action potentials. However, the scatter and

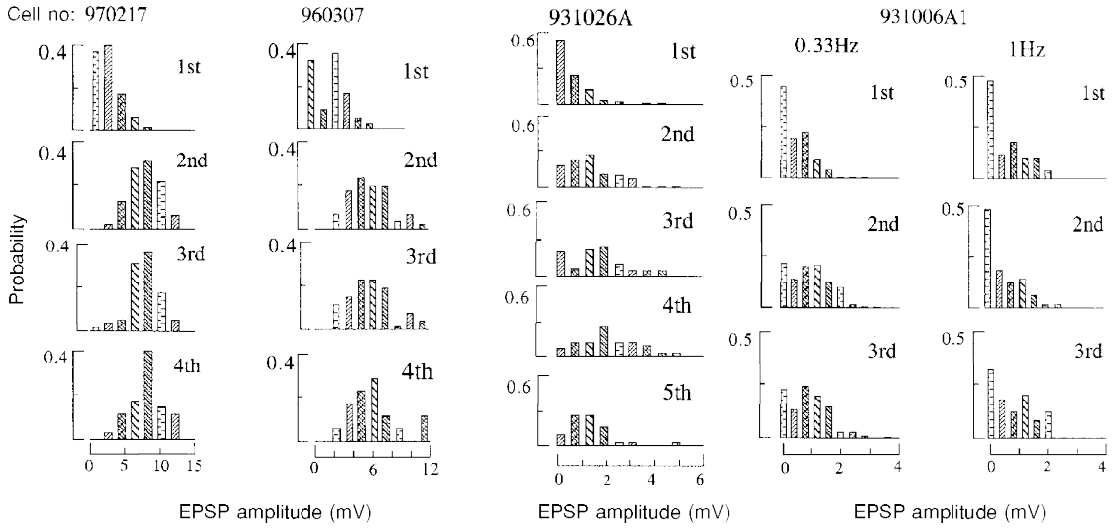

Figure 6. EPSP amplitude distributions for four pyramid to horizontal O–A interneurone connections

Single sweep EPSP amplitudes were measured under direct manual control, binned and plotted as probability distributions. Where no apparent postsynaptic response was elicited by a presynaptic spike a zero was entered. The first bin therefore represents the apparent failures of transmission in each case. Where second, third or fourth EPSPs summed with preceding EPSPs, an averaged first, second or third EPSP was scaled to match the amplitude of the equivalent single sweep event and the amplitude measured as the difference between the peak of the EPSP and the equivalent point on the decay phase of the preceding EPSP. For first EPSPs and later EPSPs that were well separated in time, the amplitude was measured as the difference between the baseline preceding the EPSP and the peak. Because these measures were necessarily controlled by hand to eliminate obvious artifacts or spontaneous events and the longest reasonable samples were used, the durations of the baseline and peak samples chosen to represent the most accurate estimates varied from event to event. Estimates of equivalent noise distributions were therefore not feasible. Because relatively few measurements are included in each histogram (70–200 for first and second EPSPs, 50–180 for third EPSPs, 20–40 for fourth and fifth EPSPs) data are coarsely binned and histograms included simply as a description of the data. The proportion of failures in response to the first presynaptic spike is greatest with the smallest EPSP (931026A, >50 %) and least with the largest EPSP (960307, <40 %). The proportion of failures decreases and the proportion of larger events increases when second, third, fourth and fifth EPSPs are compared with first EPSPs for all data sets collected at one spike burst per 3 s (0·33 Hz). At 1 Hz, however, (931006A1) second EPSPs were on average slightly smaller than first EPSPs and the proportion of failures was similar.

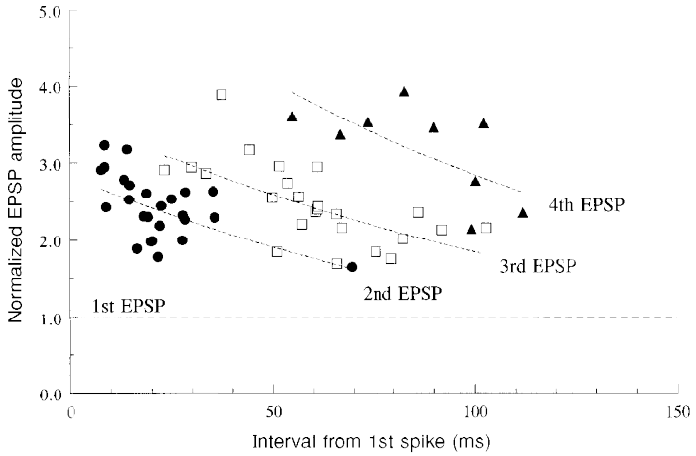

Figure 7. Normalized second, third and fourth EPSP amplitudes plotted against the time interval following the first spike in the train

Data subsets used for these points each include EPSPs recorded from a single pair, at one membrane potential and with a relatively narrow range of interspike intervals. The mean interval for each data set is plotted. The S.D.s about the mean were <4 ms for intervals <20 ms and up to 10 ms for the longest intervals. Normalized mean EPSP amplitude is plotted for each subset (n, 20–60), e.g. the mean amplitude of the second EPSP divided by the mean amplitude of the first EPSP for that subset. C.V.s for these EPSPs were large, $0{\cdot}84 \pm 0{\cdot}37$ for the first EPSPs and $0{\cdot}47 \pm 0{\cdot}24$ for second EPSPs. Double log regression lines are indicated by the dotted lines. Correlation coefficients were, however, low ($0{\cdot}7 > r > 0{\cdot}6$) and these lines simply represent the trend.

relatively small numbers of data points preclude any more detailed analysis.

Paired pulse and brief train facilitation appear to be mediated presynaptically

The EPSP amplitude distributions for four of these pairs spanning the range of average EPSP amplitudes recorded in this study, are illustrated in Fig. 6. Since only relatively small numbers of events (70–200 for first EPSPs, 20–40 for fourth and fifth EPSPs) are included in each plot, no attempt is made here to distinguish peaks and data are binned coarsely. A similar pattern was apparent in all the pairs when brief bursts of EPSPs were elicited at a rate of one per 3 s (0·33 Hz). The first EPSP amplitude distribution includes a significant proportion of apparent failures of transmission and few large events. Second and subsequent EPSP amplitude distributions display fewer, or no apparent failures and include larger events. With the exception of those that include many failures, which are of course skewed, these distributions are relatively evenly distributed about the mean, suggesting that they may not depart significantly from binomial distributions and that comparisons of the changes in c.v.$^{-2}$ and in mean amplitude (M) may indicate whether the facilitation observed was of pre- or postsynaptic origin (Faber & Korn, 1991; Thomson, Deuchars & West, 1993*a*,*b*).

In a simple binomial model of transmission, an increase in q (quantal amplitude) results in an equivalent proportional increase in M (npq), but no change in c.v.$^{-2}$ ($np/(1-p)$, where n equals the number of release sites and p the probability of release). A change in n alone results in an

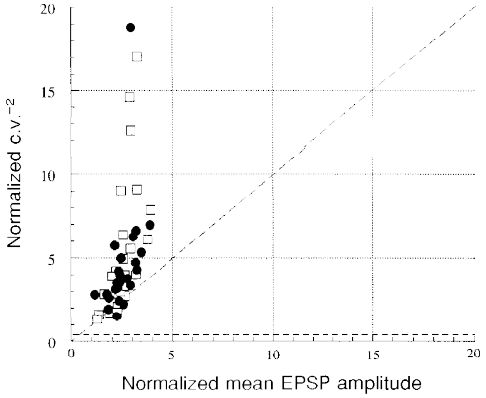

Figure 8. Normalized c.v.$^{-2}$ plotted against normalized mean EPSP amplitude for second and third EPSPs in brief trains

For each data subset (see Fig. 7 legend) mean second (●) or third (□) EPSP amplitude and c.v.$^{-2}$ were normalized using the mean and c.v.$^{-2}$ of the first EPSP for that data subset. The majority of points lie above the line of slope 1, indicating that the facilitation was due to an increase in the probability of release.

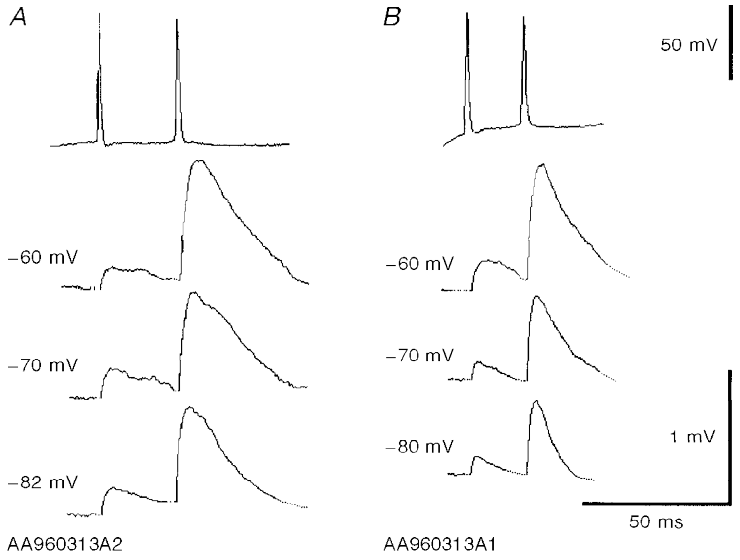

Figure 9. Comparison of two EPSPs elicited in a single horizontal O–A interneurone by two consecutively recorded pyramidal cells (*A* and *B*)

Both EPSPs increased in amplitude and duration with postsynaptic depolarization, despite their different time course at any one membrane potential. Paired pulse facilitation was apparent in both connections at all 3 membrane potentials.

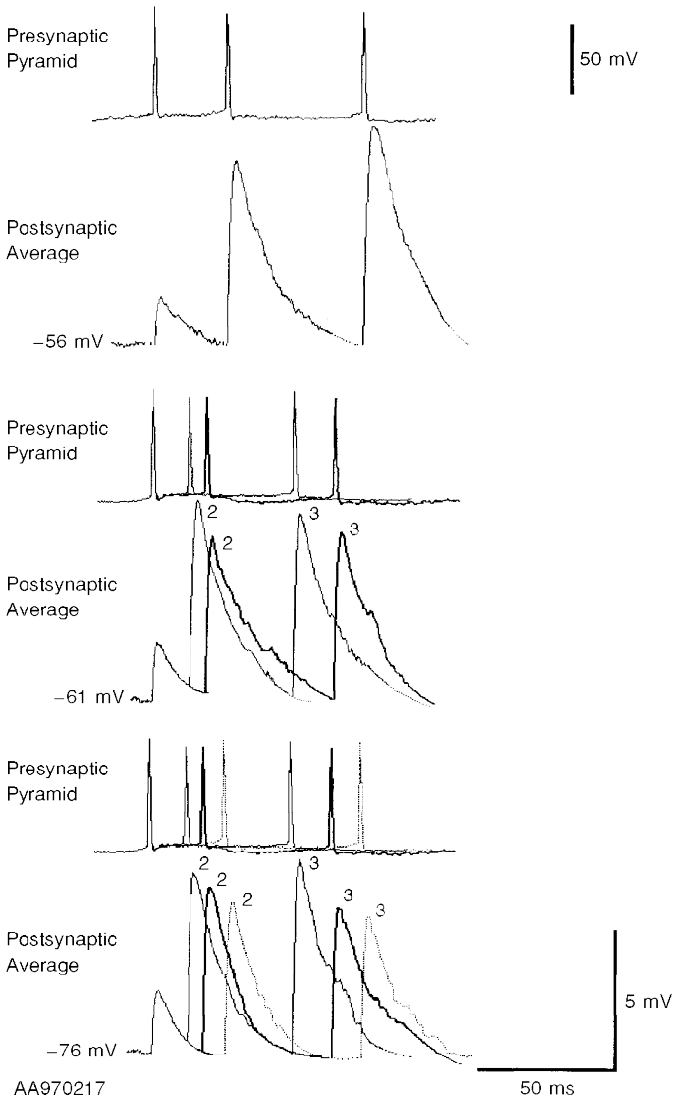

Figure 10. EPSPs in a pyramid to horizontal O–A interneurone connection generated by brief spike trains of different durations and recorded at different postsynaptic membrane potentials

The averaged EPSPs each include between 60 and 120 single sweeps. EPSPs elicited by brief trains of 3 presynaptic spikes were recorded at 3 different postsynaptic membrane potentials (−56, −61 and −76 mV). At −76 mV averaged responses to spike trains of 3 different durations are compared. The facilitation of the second and third EPSPs appears to decline with increasing interspike interval. A similar time dependence is apparent at −61 mV, where averaged responses to spike trains of 2 durations are compared. At −56 mV, maximal second and third EPSP facilitation at the briefest interspike intervals resulted in postsynaptic action potentials, so only the averaged response to the longest (slowest) train is illustrated. Comparison of EPSPs elicited by spike trains of similar duration indicates that the EPSPs increased in amplitude with postsynaptic depolarization.

equivalent proportional change in both M and c.v.$^{-2}$, while a change only in p results in a greater proportional change in c.v.$^{-2}$ than in M. As illustrated in Fig. 8, in the majority of data subsets, facilitation of the second and third EPSPs was associated with a larger proportional increase in c.v.$^{-2}$ than in M, indicating that this facilitation involves an increase in the probability of release.

In only one data subset, obtained when bursts were elicited at a rate of one per second (see Fig. 6, cell no. 931006A1, 1 Hz), was the proportion of apparent failures in the second EPSP distribution similar to that of the first, and at 1 Hz the paired pulse facilitation that had been apparent at 0·33 Hz was replaced by a slight paired pulse depression after 5 min.

Voltage relations of EPSPs in horizontal O–A interneurones

To determine whether the facilitation described here was influenced by postsynaptic membrane potential, four of the EPSPs were recorded at three or four different postsynaptic membrane potentials. In three, the averaged EPSP increased in amplitude with depolarization with a concomitant small increase in duration (Figs 9 and 10). The large c.v.s of the first EPSPs, precluded further analysis of voltage-dependent changes in first EPSP amplitude, but the consistency in the changes for second (Fig. 9) and third EPSPs and EPSPs elicited at different interspike intervals (see Fig. 10) indicates a trend, i.e. that these EPSPs increase in both amplitude and duration with membrane depolarization. In the remaining pair, the EPSP increased slightly in amplitude and duration with depolarization from −78 to −72 mV, but with further depolarization decreased again (Fig. 11). The averaged second and third EPSPs recorded at −61 and −69 mV may, however, be underestimates of mean amplitude since the largest single sweep EPSPs activated postsynaptic action potentials at this membrane potential and were excluded from the analysis (see Fig. 12). Despite these changes in amplitude

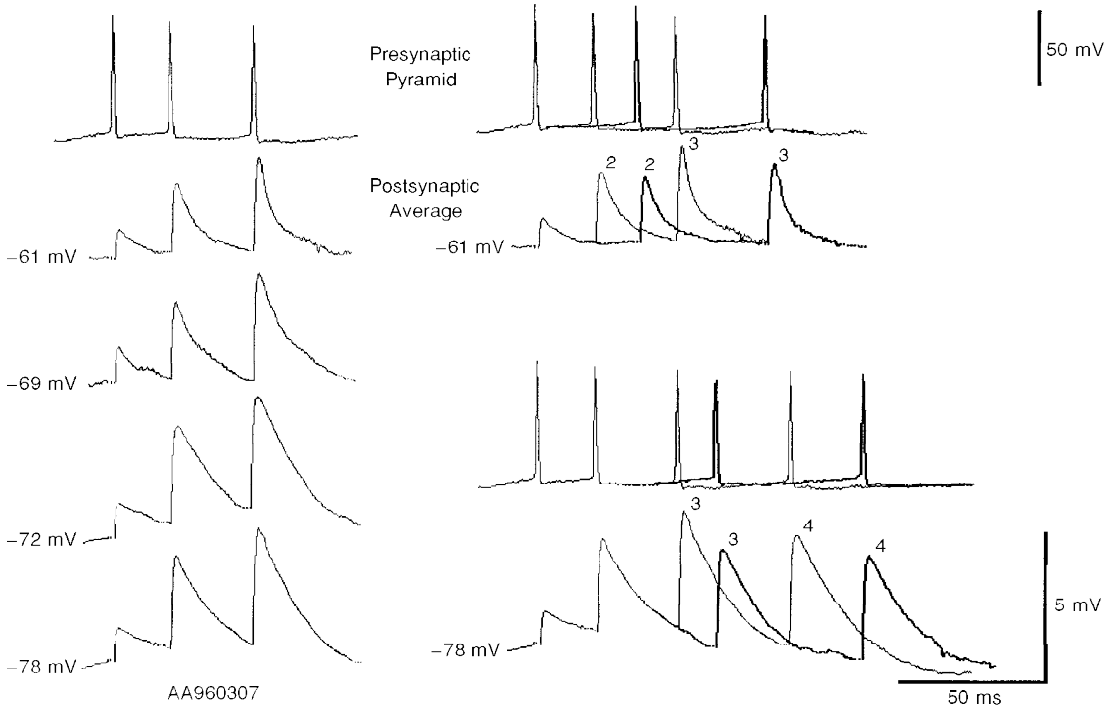

Figure 11. EPSPs in a pyramid to horizontal O–A interneurone connection generated by brief spike trains of different durations and recorded at different postsynaptic membrane potentials

The averaged EPSPs each include between 60 and 120 single sweeps. On the left, EPSPs elicited by similar, brief trains of 3 presynaptic spikes were recorded at 4 different postsynaptic membrane potentials (−61, −69, −72 and −78 mV). Averaged EPSPs decreased in amplitude and duration with hyperpolarization to −78 mV and with depolarization to −69 mV from −72 mV. This latter decrease in amplitude may, however, be an overestimate as at −69 and −61 mV the largest single sweep events elicited postsynaptic action potentials (see Fig. 12) and were excluded from the analysis. Paired pulse and brief train facilitation are, however, apparent and relatively similar at all membrane potentials. On the right, responses to brief 3 and 4 spike trains of different durations are compared at two membrane potentials (−61 and −78 mV). At −61 mV averaged responses to 3 spike trains of two different durations are compared. Facilitation of second and third EPSPs appear to decline with increasing interspike interval. At −78 mV averaged responses to trains of 4 spikes in which the timing of the third and fourth (but not the second) presynaptic spikes are different, are compared. Facilitation of the third and fourth EPSPs appears to decline with increasing interspike interval.

and duration with membrane potential, however, paired pulse and brief train facilitation were apparent at all membrane potentials and were relatively similar in degree, when the variability of these events is taken into account.

DISCUSSION

The properties of excitatory connections from pyramidal cells to horizontal O–A interneurones are described here. The two most distinctive features of these interneurones were the profound 'sag' in the response to hyperpolarizing current which is probably indicative of I_h (or Q-current) (Lacaille & Williams, 1990; Maccaferri & McBain, 1996) and the precision of their axonal targeting of s. lacunosum-moleculare (e.g. Sík *et al.* 1995). Horizontal O–A interneurone action potentials were brief, showed little spike frequency accommodation and adaptation and were terminated by a large, rapid onset spike AHP.

Paired pulse and brief train facilitation at pyramid to horizontal O–A interneurone connections

Pyramid to horizontal O–A interneurone connections consistently displayed paired pulse and brief train facilitation that was frequency dependent. This pattern was qualitatively similar to that previously described for pyramidal inputs onto classical fast spiking and onto burst firing interneurones in neocortex (Thomson *et al.* 1993*a*, 1995; Thomson, 1997), but was less pronounced. The facilitation, particularly at inputs onto classical fast spiking cells in neocortex could reach 30 times. Moreover, to raise release probability for first spikes sufficiently to switch the release pattern from facilitation to depression, these neocortical synapses required repeated bursts at 1 s^{-1} for 20 min in raised extracellular Ca^{2+} (5 mM). In the present study, a much less dramatic protocol was required to enhance first EPSPs and to initiate the switch from facilitation to depression (1 burst per second for 5–10 min in normal, 2·5 mM Ca^{2+}), indicating that release probability under the present experimental conditions, though lower than for inputs onto bistratified and basket cells and onto other pyramidal cells, is not as low as at some neocortical synapses. It should, perhaps, be noted that these changes in release probability initiated by repeated bursts at one per second are not long lasting. Following a return to one per 3 s the original pattern reemerges within a few minutes.

The facilitation is probably at least in part of presynaptic origin, since apparent failures of transmission were frequently seen following single spikes, but less frequently following second, third or fourth spikes (cf. Stevens & Wang, 1995). Coefficient of variation analysis also indicated a presynaptic site of origin for at least a significant proportion of the facilitation of second and third EPSPs. The low probability of release at 0·33 Hz could be due to insufficient calcium influx during the first presynaptic action potential. Calcium entry during a second or a third action potential may, however, reach threshold for transmitter release at a release site that has already bound some Ca^{2+} (Stanley, 1995), resulting in facilitation.

The mechanisms underlying the rather different release properties of the different terminals of CA1 pyramidal axons remain to be elucidated. At terminals onto horizontal O–A interneurones there is an apparently low probability for release and brief train facilitation results. In contrast, pyramidal axon synapses onto basket cells, bistratified interneurones (see Ali *et al.* 1998) and other pyramids (Thomson *et al.* 1993*b*; Deuchars *et al.* 1994; Deuchars & Thomson, 1996) display a higher release probability and

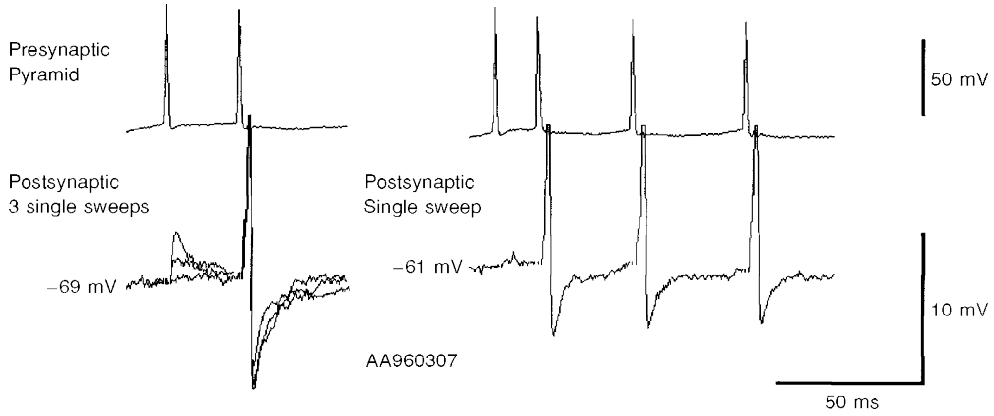

Figure 12. Postsynaptic spikes

At membrane potentials less negative than −69 mV, second, third and fourth EPSPs (but very rarely first EPSPs) in brief trains could trigger postsynaptic spikes in this interneurone. This figure illustrates the short and constant latencies of these postsynaptic spikes, although the spike AHP varied from sweep to sweep. On the left, 3 single sweep responses to pairs of presynaptic spikes are superimposed. On the right a single sweep response to a train of 4 presynaptic spikes is shown. Sweeps including postsynaptic spikes were excluded from the averaged EPSPs illustrated in other figures.

brief train depression results. Pyramidal terminals on horizontal O–A interneurones have a uniquely high concentration of mGluR7 in the presynaptic grid (Shigemoto *et al.* 1996). There is therefore at least one structural difference between the synapses formed by pyramidal cells with horizontal O–A interneurones and those formed with all other postsynaptic targets. Moreover, similar differences in the patterns of transmitter release at terminals of the same presynaptic axon on different postsynaptic targets have been reported in neocortex (Thomson, 1997) and in invertebrate models (e.g. Katz *et al.* 1993).

Voltage relations of EPSPs

Three of four EPSPs recorded at several postsynaptic membrane potentials increased in amplitude and duration with depolarization. Preliminary studies indicate that this increase may involve NMDA receptors and the non-linearity of the NMDA receptor-mediated voltage relation may account for the slight enhancement of strongly facilitated second EPSPs at the more depolarized potentials compared with first EPSPs and with second EPSPs at more negative potentials (e.g. Fig. 9*A*). One of the EPSPs decreased in both amplitude and duration (Fig. 11). The origin of this decrease has not been determined, but might involve activation of voltage-dependent outward currents. Paired pulse and brief train facilitation was, however, apparent at all membrane potentials between −80 mV and spike threshold.

Morphology and the position of horizontal O–A interneurones in the local circuit

Eight of the ten horizontal O–A interneurones were fully reconstructed at the light microscopic level and were similar to those described previously (Ramón y Cajal, 1911; Sík *et al.* 1995; for review see Freund & Buzsáki, 1996). The

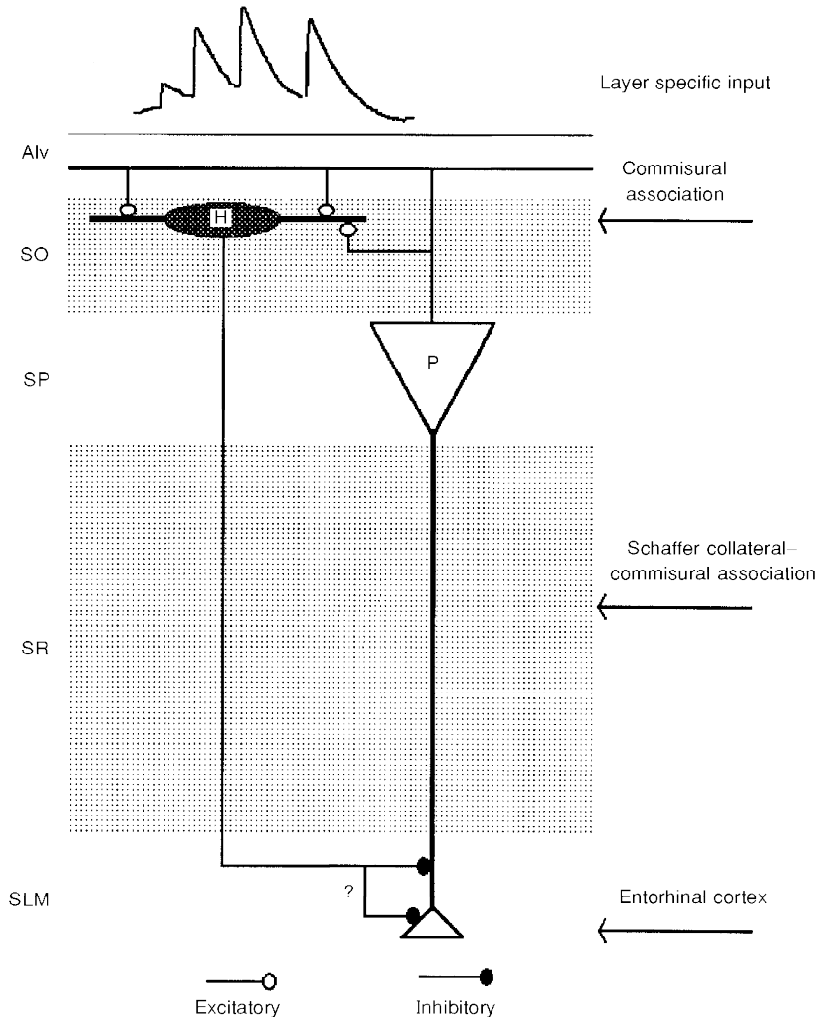

Figure 13. Summary diagram of the dendritic and axonal arborization and possible synaptic contacts made and received by a horizontal O–A interneurone

A pyramidal cell directly excites a horizontal O–A interneurone, which might then suppress inputs from entorhinal cortex to that pyramidal cell by shunting current in distal dendrites.

electrophysiological characteristics of the other two cells were similar and distinctly different from those of other cell types in the region. In two longitudinally cut slices the dendrites of the horizontal O–A interneurones recovered extended further along the O–A border (see Fig. 4) than those of interneurones recorded from transverse sections (Figs 3 and 5). One of these cells also gave rise to the largest EPSPs recorded (the other was not recorded as a postsynaptic partner). It is possible therefore that only a part of the dendritic tree of these cells is maintained in traditional transverse sections, and that some of the input from CA1 pyramids is missing in 450–500 μm thick sections. However, the axonal arborization of the O–A interneurone was limited in this longitudinal plane of section, suggesting that the axons and dendrites of these cells may extend in somewhat different planes. Thus the strikingly strong inputs from CA1 pyramidal cells reported here (probability 1:3, single sweep amplitude up to 2–12 mV) may even be an underestimate of the connectivity *in vivo*. This illustrates how powerfully these interneurones are innervated by CA1. The powerful excitatory drive that horizontal O–A interneurones receive from pyramidal cells and their selective innervation of s. lacunosum-moleculare, which receives entorhinal cortex input, places them in a unique feedback position in the local circuit. Other interneurones in CA1 receive less powerful inputs from CA1 and innervate different regions of pyramidal cells.

Figure 13 is a schematic of the local circuit involving a horizontal O–A interneurone. A pyramidal cell directly excites a horizontal O–A interneurone, which could in turn suppress inputs from the entorhinal cortex to that pyramidal cell and its neighbours by shunting current in distal dendrites. Although preliminary studies (Samulack & Lacaille, 1993; Yanovsky *et al.* 1997) indicate that both $GABA_A$ and $GABA_B$ receptors are involved in the inhibition of distal pyramidal dendrites by these interneurones, the detailed properties of these inhibitory connections in s. lacunosum moleculare remain to be determined. Clearly, however, the synchronous high frequency discharge in a population of pyramidal cells that occurs, for example, during theta rhythm, would greatly facilitate recruitment of these interneurones and in turn modify entorhinal cortex input to CA1. The extent to which these synapses would facilitate during repetitive, high frequency presynaptic bursts would depend on the duration of theta activity, the number of spikes in each burst, in each presynaptic cell and the interburst intervals. It is possible, for instance, that the facilitation generated by one burst of four of more spikes would not have declined completely before the next burst began and that the horizontal interneurones might be activated earlier and earlier in the cycle as theta activity continued.

Ali, A. B., Deuchars. J., Pawelzik, H. & Thomson, A. M. (1998). CA1 pyramidal to basket and bistratified cell EPSPs: dual intracellular recordings in rat hippocampal slices. *Journal of Physiology* **507**, 201–217.

Ali, A. B. & Thomson, A. M. (1996). Pharmacology of CA1 pyramid to oriens alveus interneurone connections in rat hippocampus. *Society for Neuroscience Abstracts* **317**, 1.

Ali, A. B. & Thomson, A. M. (1997). Brief train depression and facilitation at pyramid–interneurone connections in slices of rat hippocampus; paired recordings with biocytin filling. *Journal of Physiology* **501.P**, 9*P*.

Blasco-Ibanez, J. M. & Freund, T. F. (1995). Synaptic input of horizontal interneurones in stratum oriens of the hippocampal CA1 subfield: structural basis of feedback activation. *European Journal of Neuroscience* **7**, 2170–2180.

Buckmaster, P. S., Kunkel, D. D., Robbins, R. J. & Schwartzkroin, P. A. (1994). Somatostatin-immuno-reactivity in the hippocampus of mouse, rat, guinea pig and rabbit. *Hippocampus* **4**, 167–180.

Buhl, E. H., Halasy, K. & Somogyi, P. (1994). Diverse sources of hippocampal unitary inhibitory postsynaptic potentials and the number of release sites. *Nature* **368**, 823–828.

Buhl, E. H., Han, Z.-S., Lorinczi, Z., Stezhka, V. V., Karnup, S. V. & Somogyi, P. (1994). Physiological properties of anatomically identified axo-axonic cells in rat hippocampus. *Journal of Neurophysiology* **71**, 1289–1306.

Buhl, E. H., Szilágyi, T., Halasy, K. & Somogyi, P. (1996) Physiological properties of anatomically identified basket and bistratified cells in the CA1 area of the rat hippocampus *in vitro*. *Hippocampus* **6**, 1–10.

Deuchars, J. & Thomson, A. M. (1996). CA1 pyramid–pyramid connections in rat hippocampus *in vitro*: dual intracellular recordings with biocytin filling. *Neuroscience* **74**, 1009–1018.

Deuchars, J., West, D. C. & Thomson, A. M. (1994). Relationships between morphology and physiology of pyramid–pyramid single axon connections in rat neocortex *in vitro*. *Journal of Physiology* **478**, 423–435.

Faber, D. S. & Korn, H. (1991). Applicability of the coefficient of variation method for analyzing synaptic plasticity. *Biophysics Journal* **60**, 1288–1294.

Freund, T. F. & Buzsáki, G. (1996). Interneurones in the hippocampus. *Hippocampus* **6**, 345–470.

Gulyás, A. I., Miles, R., Hájos, N. & Freund, T. F. (1993). Precision and variability in postsynaptic target selection of inhibitory cells in the hippocampal CA3 region. *European Journal of Neuroscience* **5**, 1729–1751.

Halasy, K., Buhl, E. H., Lorinczi, Z., Tamas, G. & Somogyi, P. (1996). Synaptic target selectivity and input of GABAergic basket and bistratified interneurones in the CA1 area of the rat hippocampus. *Hippocampus* **6**, 306–329.

Katz, P. S., Kirk, M. D. & Govind, C. K. (1993). Facilitation and depression at different branches of the same motor axon: evidence for presynaptic differences in release. *Journal of Neuroscience* **13**, 3075–3089.

Kosaka, T., Wu, J.-Y. & Benoit, R. (1988). GABAergic neurones containing somatostatin-like immunoreactivity in the rat hippocampus and dentate gyrus. *Experimental Brain Research* **71**, 388–398.

Kunkel, D. D. & Schwartzkroin, P. A. (1988). Ultrastructural characterization and GAD co-localization of somatostatin-like immunoreactive neurons in CA1 of rabbit hippocampus. *Synapse* **2**, 371–381.

Lacaille, J.-C., Mueller, A. L., Kunkel, D. D. & Schwartzkroin, P. A. (1987). Local circuit interactions between oriens/alveus interneurones and CA1 pyramidal cells in hippocampal slices: electrophysiology and morphology. *Journal of Neuroscience* **7**, 1979–1993.

Lacaille, J.-C. & Williams, S. (1990). Membrane properties of interneurones in stratum oriens-alveus of the CA1 region of rat hippocampus *in vitro*. *Neuroscience* **36**, 349–359.

Li, X.-G., Somogyi, P., Tepper, J. M. & Buzsáki, G. (1992). Axonal and dendritic arborization of an intracellularly labelled chandelier cell in the CA1 region of rat hippocampus. *Experimental Brain Research* **90**, 519–525.

McBain, C. J. (1994) Hippocampal inhibitory neurone activity in the elevated potassium model of epilepsy. *Journal of Neurophysiology* **72**, 2653–2863.

McBain, C. J., Dichiara, T. J. & Kauer, J. A. (1994). Activation of metabotropic glutamate receptors differentially affects two classes of hippocampal interneurones and potentiates excitatory synaptic transmission. *Journal of Neuroscience* **14**, 4433–4445.

Maccaferri, G. & McBain, C. J. (1995). Passive propagation of LTD to stratum oriens-alveus inhibitory neurons modulates the temporoammonic input to the hippocampal CA1 region. *Neuron* **15**, 137–145.

Maccaferri, G. & McBain, C. J. (1996) The hyperpolarization-activated current (I_h) and its contribution to pacemaker activity in rat CA1 hippocampal stratum oriens–alveus interneurones. *Journal of Physiology* **497**, 119–130.

Markram, H. & Tsodyks, M. (1996). Redistribution of synaptic efficacy between neocortical pyramidal cells. *Nature* **382**, 807–810.

Miles, R., Tóth, K. & Gulyás, A. I., Hájos, N. & Freund, T. F. (1996). Differences between somatic and dendritic inhibition in the hippocampus. *Neuron* **16**, 815–823.

Morrison, J. H., Benoit, R., Magistretti, P. J., Ling, N. & Bloom, F. E. (1982). Immunocytochemical distribution of pro-somatostatin-related peptides in hippocampus. *Neuroscience Letters* **34**, 137–142.

Ramón y Cajal, S. (1911). *Histologie de systeme nerveux de l' Homme et des vertebres*, tomme II. Maloine, Paris.

Samulack, D. D. & Lacaille, J.-C. (1993). Hyperpolarizing synaptic potentials evoked in CA1 pyramidal cells by glutamate stimulation of interneurones from the oriens/alveus border of rat hippocampal slices. II. Sensitivity to GABA antagonists. *Hippocampus* **3**, 345–358.

Shigemoto, R., Kulik, A., Roberts, J. D. B., Ohishi, H., Nusser, Z., Kaneko, T. & Somogyi, P. (1996). Target-cell-specific concentration of a metabotropic glutamate receptors in the presynaptic active zone. *Nature* **381**, 523–525.

Sík, A., Penttonen, M., Ylinen, A. & Buzsáki, G. (1995). Hippocampal CA1 interneurones: an *in vivo* intracellular labelling study. *Journal of Neuroscience* **15**, 6651–6665.

Stanley, E. F. (1995). Calcium entry and the functional organization of the presynaptic transmitter release site. In *Excitatory Amino Acids and Synaptic Transmission*, 2nd edn, ed. Wheal, H. V. & Thomson, A. M., pp. 17–27. Academic Press, London.

Stevens, C. F. & Wang, Y. (1995). Facilitation and depression at single central synapses *Neuron* **14**, 795–802.

Thomson, A. M. (1997). Activity-dependent properties of synaptic transmission at two classes of connections made by rat neocortical pyramidal axons *in vitro*. *Journal of Physiology* **502**, 131–147.

Thomson, A. M., Deuchars, J. & West, D. C. (1993*a*). Single axon excitatory postsynaptic potentials in neocortical interneurones exhibit pronounced paired pulse facilitation. *Neuroscience* **54**, 347–360.

Thomson, A. M., Deuchars, J. & West, D. C. (1993*b*). Large, deep layer pyramid–pyramid single axon EPSPs in slices of rat motor cortex display paired pulse and frequency-dependent depression, mediated presynaptically and self-facilitation, mediated postsynaptically. *Journal of Neuroscience* **70**, 2354–2369.

Thomson, A. M., West, D. C. & Deuchars, J. (1995). Properties of single axon excitatory postsynaptic potentials elicited in spiny interneurones by action potentials in pyramidal neurones in slices of rat neocortex. *Neuroscience* **69**, 727–738.

Toth, K., Borhegyi, Z. & Freund, T. F. (1993). Postsynaptic targets of GABAergic hippocampal neurons in the medial septum-diagonal band of Broca complex. *Journal of Neuroscience* **13**, 3712–3724.

Toth, K. & Freund, T. F. (1992). Calbindin D28k-containing non-pyramidal cells in the rat hippocampus: their immunoreactivity for GABA and projection to the medial septum. *Neuroscience* **49**, 793–805.

Yanovsky, Y., Sergeeva, O. A., Freund, T. F. & Haas, H. L. (1997). Activation of interneurones at the stratum oriens/alveus border suppresses excitatory transmission to apical dendrites in CA1 area of the mouse hippocampus. *Neuroscience* **77**, 87–96.

Zhang, L. & McBain, C. J. (1995*a*). Voltage-gated potassium currents in stratum oriens–alveus inhibitory neurones of the rat CA1 hippocampus. *Journal of Physiology* **488**, 647–660.

Zhang, L. & McBain, C. J. (1995*b*). Potassium conductances underlying repolarization and afterhyperpolarization in rat CA1 hippocampal interneurones. *Journal of Physiology* **488**, 661–672.

Acknowledgements

We would like to thank Norvartis Pharma (Basel), The Medical Research Council and The Wellcome trust for financial support. A. Ali is a Norvartis Pharma (Basel) funded student.

Corresponding author

A. M. Thomson: Department of Physiology, Royal Free Hospital School of Medicine, Rowland Hill Street, London NW3 2PF, UK.

Authors' email addresses

A. M. Thompson: alext@rfhsm.ac.uk

A. B. Ali: aali@rfhsm.ac.uk